FOREX Publication
Open Access | Rapid and quality publishing

International Journal of
Electrical and Electronics Research (IJEER)
Research Article | Volume 10, Issue 3 | Pages 579-584 | e-ISSN: 2347-470X

Enhanced Classification of Faults of Photovoltaic Module Through Generative Adversarial Network

S. Bharathi[1] and P. Venkatesan[2]

[1]*Research Scholar, SCSVMV University, Kanchipuram, Tamil Nadu, India, bharathieee@kanchiuniv.ac.in*
[2]*Associate Professor, SCSVMV University, Kanchipuram, Tamil Nadu, India, venkatesan.p@kanchiuniv.ac.in*

***Correspondence:** S. Bharathi; Email: bharathieee@kanchiuniv.ac.in

ABSTRACT- The faults occurring in the photo voltaic system has to be detected to make it work efficiently .To detect and classify the faults occurring in the photo voltaic module infrared images, electro luminescent images, photo luminescent images of photo voltaic module is used .Using infrared images around 11 faults of photovoltaic module such as cell ,cell-multi, hot-spot-multi , hot-spot, cracking, diode, diode-multi, vegetation, shadowing, off-line module and soiling faults can be detected. In addition to the original infra-red images (IR) available in the IR dataset, the IR images are generated for each and every category of faults by using generative adversarial networks (GAN's) to increase the dataset size. 45000 images are generated by GAN's. Later the images are used to train and test the convolution neural network. The dataset visualization of original and that of GAN generated images are done in 2-dimensional space using uniform manifold approximation and projection. In this work 12 categories of IR dataset are considered for classification in which 11 belongs to fault category and the remaining one is the normal category of images. In earlier work only 11 category of faults or less than that is considered for classification. Compared the results with the existing work and it is found that by enhancing the dataset size by GAN's accuracy of 91.7 % is obtained during the classification of 8 categories of faults.

Keywords: Uniform Manifold Approximation and Projection (UMAP), MPPT, GAN's, IR images, CNN.

ARTICLE INFORMATION
Author(s): S. Bharathi and P. Venkatesan
Received: 25/06/2022; **Accepted**: 15/08/2022; **Published**: 07/09/2022;
e-ISSN: 2347-470X;
Paper Id: IJEER220634;
Citation: 10.37391/IJEER.100328
Webpage-link:
https://ijeer.forexjournal.co.in/archive/volume-10/ijeer-100328.html

Publisher's Note: FOREX Publication stays neutral with regard to Jurisdictional claims in Published maps and institutional affiliations.

1. INTRODUCTION

Now a day's photo voltaic module is used to produce electrical power, so fault occurring in the module has to be detected well in advance before it degrades the efficiency. Electroluminescent images are obtained by giving supply to PV system and then the images are taken. In thermal imaging method the intensity of heat distribution across the PV module is obtained, using these images fault prediction is carried out. In [1] Perceptron neural network is used to classify line to line fault, open circuit condition and normal condition. Each category is assigned a range of values for current, voltage and illumination through which classification is done. They utilized 80 % of data for training and 20% of the data for testing. In [2] classification is done to identify the micro crack, break and finger interruption and normal condition in EL images of PV system. Data augmentation is performed by them to elevate the size of the dataset and to improve the classifier performance. The RMS Prop optimization algorithm is employed for classification. Kernel size is varied and the performance metrics are evaluated for each case. In [3] PV cell defects are classified by training CNN with 80% of dataset and 20 % of data is used for testing, the loss function used by the CNN classifier is the cross entropy.

In [4] EL and IR image of photo voltaic module is used by them. pre training of the CNN is done with EL images and then it is trained with IR images, cell cracking, failed cell interconnection and failed/resistive soldering bonds are classified by them. In [5] the data set consisting of infrared images of 11 categories of faulty and also normal images is taken from the infrared solar module dataset. Data augmentation techniques are performed on the IR images and faults are classified by the CNN model. In [6] a PV cell connected to a maximum power point tracking and buck boost converter circuit is considered by them. The parameters such as irradiance, Temperature, Fault impedance, percentage of mismatch, percentage of partial shading and high impedance applied to a PV cell is varied. The value of current and voltage are noted from the circuit during line-to-line fault and at 25 degrees Celsius. 1D parameters are converted in to 2D scalogram and a CNN is pre trained using them. The features extracted from CNN are classified by SVM and RF classifiers. the fine tuning of the pre training is done and classification is performed with it. In [7] Defects such as micro crack, in active region, grid line, material and back ground defects are classified using EL image dataset. Accelerated stress test, post SMLT test, pos HF10 and post HF20 are the tests carried out by manufacturing company of photovoltaic module. They observed that the performance is more while detecting cell spacing and ribbon interconnection and during the classification of gridline and crack. In [11] 11 parameters are obtained through the sensors connected to the experimental setup. Feature reduction and optimal values of the parameters of the classifiers are obtained by them using grid search function. Ensemble models are used by them for classification. The

FOREX Publication
Open Access | Rapid and quality publishing
International Journal of Electrical and Electronics Research (IJEER)
Research Article | Volume 10, Issue 3 | Pages 579-584 | e-ISSN: 2347-470X

number of faults classified by them is 4. In [12] A threshold is assigned for open circuit string, short circuit string and fault free operation based on which fault detection is carried out by them.

Table 1: The data available in the IR dataset (in row1) and since it is highly imbalanced the images are produced for each category through GAN's (row 2) and 5000 images for each category is given as input to CNN.

Dataset (IR image)	Defect free image	Number of defective images										
		Cell	Cell-Multi	Cracking	Hot spot	Hot spot multi	Diode	Diode-multi	Offline Module	Soiling	Shadowing	Vegetation
Dataset (IR image)	10000	1877	1288	940	249	246	1499	175	827	204	1056	1639
Images through GAN's	-	3123	3712	4060	4751	4754	3501	4825	4173	4796	3944	3361
Total image applied to CNN	5000	5000	5000	5000	5000	5000	5000	5000	5000	5000	5000	5000

In [13] MATLAB simulation of 6 X 5 array of PV cell is carried out and characteristic curves are obtained for six different faults by considering single fault at a time. In [14] the surface defects are detected by training CNN with R, G and B components separately and finally combined the CNN outputs and applied to fully connected layer after performing dropout it is applied to soft max classifier. In [15] 4 classes of defect probability is considered and it is classified by mobile net v2, inception v3, resnet- 50 and resnet-50 with modification. In [16] drone with charge coupled device and thermal camera video of solar plant is taken and the frames are segmented to detect hotspot in the image through morphological processing techniques .In [17] a SCADA system is incorporated in the power plant and data is collected from it . In [18] the features under healthy and shading module conditions are obtained by them through experimental set up. The features are then classified using Principal Component Analysis (PCA). The drawback of CNN is that more images are required to yield fruitful classification results. So, the infrared images from each category of fault in the data set are used to train GAN's to generate images and the size of the dataset is increased very much. Then the preprocessing is carried out to reshape the image. Then the images are visualized in UMAP embedding. The preprocessed images are applied to CNN for performing classification.

2. METHODOLOGY

Data set imbalance will degrade the performance of CNN, so GAN's are used for image generation. Visualization of the dataset is done in low dimensional space using UMAP. Later classification of images is done using CNN. The novelty in this work is that 12 categories of images are considered for classification. The infrared images from each category of fault in the original data set are used to train GAN's and the size of the dataset is increased by 45000 images. Then the preprocessing is carried out to reshape the image. The preprocessed images are applied to CNN for performing classification. The images are visualized in low dimensional UMAP embedding.

2.1 Dataset

IR images are taken from the link https://github.com/RaptorMaps/*InfraredSolarModules*.12categ -ories of infra-red images are there in the dataset.11 categories belong to faults occurring in the solar module and one category consisting of 10000 normal images. The dataset is highly imbalanced, so the data set balance can be achieved through augmentation techniques or by using generative adversarial networks (GAN's). In [5] data set balance is carried out by using few augmentation techniques but in this paper ,data set balance is obtained using GAN's. The number of images for each of the fault category in the original data set is shown in first row of the *table 1*, and the number of images generated through GAN's for each of the fault category is shown in the second row of the table.

2.2 Generator Adversarial Network

Data augmentation aims to generate more images which resemble the original images. Few data augmentation techniques [5] is used to increase the size of the dataset since deep learning models produce promising results with larger dataset. GAN's and data augmentation are the methods used to increase the size of the dataset. Data augmentation is done by performing horizontal flipping, vertical flipping, rotation etc on original images in the data set. The GAN network consists of generator and discriminator. The generator tries to generate data similar to the original data by getting noise as the input. The input noise is referred as the latent vector. The discriminator's input may be from original dataset or from the generator generated fake data. The discriminator tries to identify whether the input data given to it is real or fake. The discriminator is nothing but a classifier. The generator and the discriminator work in such a way to minimize their loss functions respectively. Initially the generator will be generating an irrelevant output, in the course of time it tries to generate data resembling the original data. In the same way initially, the discriminator predicts the fake data as the original data, original data as fake data later on it learns well and predicts correctly.

FOREX Publication
Open Access | Rapid and quality publishing
International Journal of Electrical and Electronics Research (IJEER)
Research Article | Volume 10, Issue 3 | Pages 579-584 | e-ISSN: 2347-470X

2.3 Data Visualization tool - UMAP

The data set after enhancing its size using GAN's is visualized in 2-dimensional space using UMAP. UMAP is a nonlinear method of dimensionality reduction. It starts with an assumption that the data samples applied to it are assumed to be evenly spread in a Riemannian space. The next assumption is only finite set of data points are considered in Riemannian space. Initially the Riemannian space is learnt and then lower dimensional representation is obtained in UMAP dimensionality reduction technique. A ball is formed around each data point in the high dimensional space whose radius is adjustable for each and every data points. A complex topological arrangement is made based on 0 simplex, 1 simplex etc. The probability with which an edge connects two data points is determined in the high dimensional space then the directional probabilities a and b of an edge is calculated using a + b- ab In low dimensional space optimization of data arrangement is done by using cross entropy and its value is calculated from *equation (1).* E consists of all possible 1-simplices, the weight function w_h (e) is the weight associated with the 1-simplex e in the high dimensional case and the weight associated with the 1 simplex of e in the low dimensional case is w_l (e), then the cross entropy is found using *equation (1).*

Cross entropy=

$$\sum_{e\in E}\left(w_h(e)\right)\left(log\frac{\left(w_h(e)\right)}{\left(w_l(e)\right)}\right) + \left(1-w_h(e)\right)\left(log\frac{\left(1-w_h(e)\right)}{\left(1-w_l(e)\right)}\right) \qquad (1)$$

w_h(e) provides an attractive force between the 1-simplex e if there is a large weight in the high dimensional case. The first term of the equation will be minimized when w_l(e) is high, this indicates that the distance between the points is very small in the low dimensional case. The next term represents the repulsive force between the 1-simplex e when w_h(e) is low. This is because the term will yield low value if w_l(e) as small as possible. On balance of the repulsive and attractive force, using the weights of 1-simplex edges of the high dimensional data, then the low dimensional data to settle into a state that accurately indicates the overall complex topology of the original data. Its value will be low if the distribution of probability in low dimension is far away from the distribution of probability in high dimension. Stochastic gradient is applied to the cross-entropy curve. The two parameters which highly influence the performance of UMAP is the number of nearest neighbors and minimum distance with which the data point is moved towards or away from another data point in the low dimensional graph. The input to the UMAP is 60000 images of 64 X 64 size and the visualization is done in 2-dimensional space through spectral embedding. Considering all the categories of faults.

Figure 1 shows the representation of 12 categories of faults in the 2-dimensional space and it also shows that the fault classes are highly separated in the low dimensional space

Figure 1: UMAP embedding for twelve faults

2.4 Convolution Neural Network

Convolution is performed to extract features from the image. This convolution is carried out by using a kernel and this kernel overlaps with the image. An element-wise multiplication of kernel element with the image pixel is found and later they are summed up to obtain the filtered response in the respective position of the feature map. In max pooling patches are formed in the feature maps and the maximum value in each and every patch is alone considered for further processing and the remaining values are neglected. A cost expression measures the matching between predictions of the CNN by forward pass and given target labels. The CNN network is trained with a training set of 80% of the data and it is tested with 20% of data.

2.4.1 Convolution Layer

The kernel is a matrix of size 3 X 3, 5 X 5 etc. The kernel element may contain 1, 0 etc. as elements depending on the filtering operation. An element-wise multiplication of kernel element with the image pixel is found and later they are summed up to obtain the filtered response in the respective position of the feature map.

2.4.2 Activation layer

An activation function outputs a small value for meagre inputs, and a greater value if its input is greater than the threshold. If the inputs are greater enough, the activation function will allow it. Activation functions are capable of adding non- linearities into neural networks, because of that the neural networks can learn powerful computations.

2.4.3 ReLu layer

ReLu is a linear function which gives output same as that of input provided the input to this layer is positive. This is used to avoid the diminishing of gradient.

FOREX Publication
Open Access | Rapid and quality publishing
International Journal of Electrical and Electronics Research (IJEER)
Research Article | Volume 10, Issue 3 | Pages 579-584 | e-ISSN: 2347-470X

2.4.4 Soft Max layer

An activation function chosen in the last layer of CNN is a soft max function which is used to normalize the outputs obtained from the last fully connected layer to probabilities of target class. The soft max function acts on a vector k consisting of real numbers and it give the probability to the vector of k consisting of real values that sum to 1.the expression used to find the probability values is shown in *equation (2)*

$$\sigma(\vec{z})_i = \frac{e^{z_i}}{\sum_{j=1}^{k} e^{z_j}} \qquad (2)$$

The soft max function is used as the last layer of the CNN for multiclass classification.

2.4.5 Dense layer

a layer which is deeply connected with its previous layer that is the neurons of the layer are connected to every neuron of its previous layer.

The dataset is divided in to k folds and training is performed on the model k-1 times. During the training phase one-fold out of k folds is used for testing and remaining folds are used for training the model, then the previous test fold is moved to the training set and one-fold from train set will become the test fold during the next training phase. This is done such that each and every fold will be acting as test fold one by one during each phase of training. The scores obtained during each training phase is summed up and then average score is calculated. The experiments are carried out in Google Colab and the results of which are discussed in the following session.

3. EXPERIMENTAL RESULTS

The hyper parameters are the values specified by the user to train the model. The hyper parameter values used for CNN classification is shown in *table 2*. The visualization of the CNN model structure is shown in *figure 2*. 12 layers are present in the CNN model. The input gray image is resized to 62 X 62 before applying it to the convolution block. The convolution is performed on the input images with 32 filters and the output of convolution block is applied to the ReLu activation layer. then the activation layer outputs are fed to max pooling layer. In max pooling layer 2 X 2 patches are applied on the images and the maximum value is alone given as output. Then the max pooling layer output is given as input to the dropout layer. the dropout layer output is given as input to the flatten layer which is used to flatten the input. The flattened values are fed to the dense layer then the activation is performed with ReLu layer. The ReLu activation layer output is fed to the dense layer and finally activation is performed to obtain. the probability values for the given number of classes, whose sum will be 1. The CNN is trained for 500 epochs and the variation of training and validation accuracy of the network, the variation of training and validation loss curves are shown in *figure 3.*

3.1 Case 1

Only eight category of faults such as cell, cracking, hotspot, hotspot-multi, normal, shadowing, soiling and vegetation are considered. For each fault case 5000 images are taken. 40000 images are given as input to the CNN. Train test split is made in such a way that 80 % of images i.e., 32000 images are used for training and 20 % of images is used for testing i.e.,8000 images are used for testing the CNN model. 5-fold validation is applied on these 40000 images to classify between 8 different faults. The results obtained during each fold is shown in *Table 3.*

Table 3. Accuracy obtained at 8 faults classification

Score per Fold K-fold	Training Loss	Training Accuracy	Testing Loss	Testing Accuracy
Fold 1	0.6990	1.004	1.2411	0.9019
Fold 2	0.6911	0.9918	1.0113	0.9177
Fold 3	0.7022	1.008	1.3012	0.9002
Fold 4	0.6999	0.9901	1.4298	0.9008
Fold 5	0.7011	0.9851	1.4322	0.8999

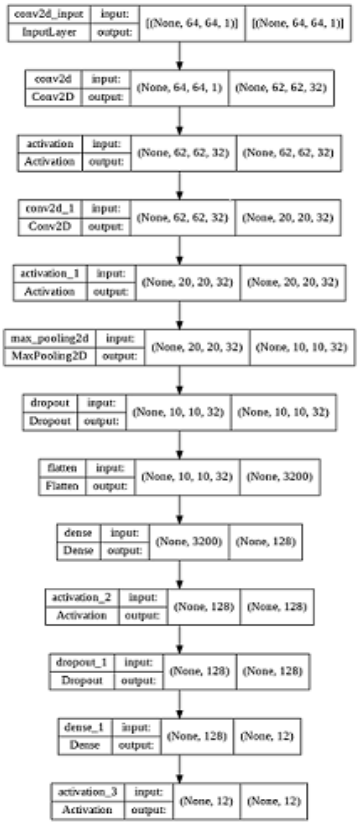

Figure 2: Flow diagram of the CNN structure used in the classification of faults in PV modules.

Table 2: Hyper Parameters used in CNN network

Number of epochs	500
Number of classes	8 for case (i) 12 for case (ii)
Batch size	32
Size of max-pooling	2
Number of filters	32
Convolution kernel size	3

FOREX Publication
Open Access | Rapid and quality publishing
International Journal of Electrical and Electronics Research (IJEER)
Research Article | Volume 10, Issue 3 | Pages 579-584 | e-ISSN: 2347-470X

3.2 Case 2

In the dataset 10000 images are available in the normal category only 5000 images are considered from it and in each of the other categories 5000 images are considered. 5000 images for a particular category of fault are obtained by fetching the images for that fault category from the original data set and the remaining images are generated using GAN's for that fault category. so, the total number of images used in this case is 60000 images. CNN model is trained with 48000 images and is tested with 12,000 images. all 12 categories of images are considered for classification by the CNN model. The CNN is trained for 500 epochs and 5-fold validation is performed. The results obtained for each and every fold is shown in *table 4*.

Table 4: Accuracy obtained at 12 faults classification

Score per Fold K-fold	Training Loss	Training Accuracy	Testing Loss	Testing Accuracy
Fold 1	0.9129	0.9604	1.5429	0.8201
Fold 2	1.9162	0.9401	2.3214	0.8103
Fold 3	1.9433	0.9318	2.3012	0.8104
Fold 4	1.9771	0.9399	2.4898	0.8099
Fold 5	0.9124	0.9569	1.5322	0.8241

The results obtained through this method is compared with that of the existing methods. In [2] EL images are trained and tested using CNN to detect four faults and the accuracy obtained by them is 0.83 during testing phase. In [5] CNN is used to classify 11 faults in IR image and the testing accuracy is 0.6373. In the proposed method 12 categories are classified with a testing accuracy of 0.824 and 8 faults are classified with a testing accuracy of 0.9177. The comparisons with existing method is shown in *table 5.*

4. CONCLUSION

The input image population size is increased using GAN by 45000, Data visualization is done in the low dimensional space using UMAP. The efficacy of the CNN increases with the data set size and it is achieved using GAN's. The novelty in this work is that the classification of 12 categories of infra-red photovoltaic images is made in this work. The CNN is trained for 500 epochs and the accuracy obtained in this work is 91.7% while classifying images of eight fault category and it is 82.4% while classifying images of 12 fault category. The limitation of this work is that the time taken for training the CNN model is very high. The new dimension of research in PV fault detection will be the detection of multiple faults occurring in single cell of the photo voltaic module. Domain adaptation aims at the classification model trained with fault images of one solar plant has to respond in the same manner to the fault images of another solar plant. Future work will be carried out in the domain adaptation field.

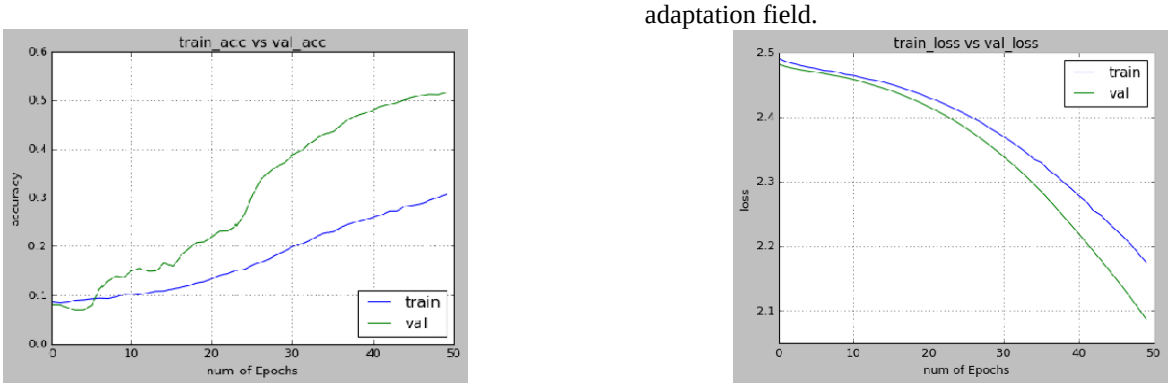

(a) (b)

Figure 3: CNN is trained till 50 epochs and the curves of (a) accuracy versus number of epochs (b) loss versus number of epochs.

Table 5: Comparison of the accuracy of different methods

Method	Number of faults	K-fold	Training Loss	Training Accuracy	Testing Loss	Testing Accuracy
CNN [2] on EL Image	4	-	-	-	-	0.83
CNN [5] on IR Image	11	Fold 3	1.2296	0.9238	2.7584	0.6373
Proposed method on IR Image	12	Fold 5	0.9124	0.9569	1.5322	**0.8241**
	8	Fold 2	0.6911	0.9918	1.0113	**0.9177**

REFERENCES

[1] Barun Basnet, Hyunjun Chun, Junho Bang, "An Intelligent Fault Detection Model for Fault Detection inPhotovoltaicSystems", Journal of Sensors, vol. 2020, ArticleID 6960328, 11 pages, 2020.

[2] Tang W., Yang Q., Xiong K., et al ,"Deep learning based automatic defect identification of photovoltaic module using electroluminescence images" Sol. Energy, 201 (2020), pp. 453-460 Ding, W. and Marchionini, G. 110107 A Study on Video Browsing Strategies. Technical Report. University of Maryland at College Park.

[3] M. Waqar Akram, Guiqiang Li, Yi Jin, Xiao Chen, Changan Zhu, Xudong Zhao, Abdul Khaliq, M. Faheem, Ashfaq Ahmad,"CNN based automatic detection of photovoltaic cell defects in electroluminescenceimages",Energy,Vol.189,2019

[4] M. Waqar Akram, Guiqiang Li, Yi Jin, Xiao Chen, Changan Zhu, Ashfaq Ahmad,Automatic detection of photovoltaic module defects in infrared images with isolated and develop-model transfer deep learning,Solar Energy,Volume 98,2020,pp. 175-186

International Journal of
Electrical and Electronics Research (IJEER)
Research Article | Volume 10, Issue 3 | Pages 579-584 | e-ISSN: 2347-470X

[5] Ricardo Henrique Fonseca Alves, Getúlio Antero de Deus Júnior, Enes Gonçalves Marra, Rodrigo Pinto Lemos,Automatic fault classification in photovoltaic modules using Convolutional Neural Networks,Renewable Energy, Volume 179, 2021, pp. 502-516.

[6] F. Aziz, A. Ul Haq, S. Ahmad, Y. Mahmoud, M. Jalal and U. Ali, "A Novel Convolutional Neural Network-Based Approach for Fault Classification in Photovoltaic Arrays," in IEEE Access, vol. 8, pp. 41889-41904, 2020.

[7] Lawrence Pratt, Devashen Govender, Richard Klein,"Defect detection and quantification in electroluminescence images of solar PV modules using U-net semantic segmentation",Renewable Energy,Vol. 178,2021,Pages 1211-1222.

[8] Antonia Creswell, Tom White, Vincent Dumoulin, Kai Arulkumaran, Biswa Sengupta and Anil A Bharath, Generative Adversarial Networks: An Overview IEEE-SPM, 2017.

[9] S. K. Firth, K. J. Lomas and S. J. Rees, "A simple model of PV system performance and its use in fault detection", Sol. Energy, vol. 84, no. 4, pp. 624-635, Apr. 2010. Brown, L. D., Hua, H., and Gao, C. 2003. A widget framework for augmented interaction in SCAPE.

[10] Y.T. Yu, M.F. Lau, "A comparison of MC/DC, MUMCUT and several other coverage criteria for logical decisions", Journal of Systems and Software, 2002, in press.

[11] McInnes et al., (2018). UMAP: Uniform Manifold Approximation and Projection. Journal of Open Source Software, 3(29), 861.

[12] Ceyhun Kapucu, Mete Cubukcu,"A supervised ensemble learning method for fault diagnosis in photovoltaic strings",Energy,Volume 227,2021

[13] Pei, T.; Hao, X. A Fault Detection Method for Photovoltaic Systems Based on Voltage and Current Observation and Evaluation. Energies 2019, 12, 1712.

[14] M. Sabbaghpur Arani, M. A. Hejazi, "The Comprehensive Study of Electrical Faults in PV Arrays", Journal of Electrical and Computer Engineering, vol. 2016, 10 pages, 2016.

[15] Chen, Haiyong, et al. "Solar cell surface defect inspection based on multispectral convolutional neural network." Journal of Intelligent Manufacturing 31.2 (2020): 453-468.

[16] Alsafasfeh, M.; Abdel-Qader, I.; Bazuin, B.; Alsafasfeh, Q.; Su, W." Unsupervised Fault Detection and Analysis for Large Photovoltaic Systems Using Drones and Machine" Vision. Energies 2018, 11, 2252.

[17] Ventura, C.; Tina, G.M. "Development of models for on-line diagnostic and energy assessment analysis of PV power plants: The study case of 1 MW Sicilian PV plant." Energy Proc. 2015, 83, 248–257.

[18] S. Fadhel, C. Delpha, D. Diallo, I. Bahri, A. Migan, M. Trabelsi, M.F. Mimouni, PV shading fault detection and classification based on I-V curve using principal component analysis: Application to isolated PVsystem,Solar Energy,Volume 179,2019,pp.1-10.

[19] Cherukuri, S. K., Kumar, B. P., Kaniganti, K. R., Muthubalaji, S., Devadasu, G., Babu, T. S., & Alhelou, H. H. (2022). A Novel Array Configuration Technique for Improving the Power Output of the Partial Shaded Photovoltaic System. IEEE Access, 10, 15056-15067.